SMALL-SCALE ATMOSPHERE-OCEAN COUPLING IN GALE-FORCE WINDS: MODELS, EXPERIMENTS, REMOTE SENSING

YU. TROITSKAYA[1,2], D. SERGEEV[1,2], A. KANDAUROV[1,2], E. EZHOVA[1,2], O.DRUZHININ[1], I.SOUSTOVA[1,2], O.ERMAKOVA[1], M.VDOVIN[1,2]

[1] Institute of Applied Physics Nizhniy Novgorod, Russia
[2] N.I. Lobachevski State University of Nizhniy Novgorod, Russia

Keywords: hurricanes, sea surface drag, spray, microwave remote sensing.

INTRODUCTION

Gale force wind at the sea represents one of the most hazardous meteorological phenomena. It is observed, first of all, under the condition of tropical cyclones. For moderate and sub-tropical parts of Europe the most dangerous storms occur due to the penetration of tropical cyclones far beyond the tropical zone. Apart from the risks for population inland, extreme storms pose a considerable threat to the safety of offshore industries, sea routes, wind technologies, oil and gas. Strong atmospheric vortices similar to tropical cyclones in genesis can be sometimes observed in mid latitudes like the quasi-tropical cyclones over the Black sea and "medicanes" over Mediterranean. In high latitudes adverse weather conditions occur during cold air advection, in Arctic fronts, and polar lows – very intensive atmospheric vortices similar to tropical cyclones in the physics of their development. The currently employed models of storms and storm surges are unsatisfactory precisely for the most severe events, where accurate modelling is the most important. One of their key shortcomings is their inability to account for the effect of the sharp drop of sea surface aerodynamic drag observed under very strong winds. Under these conditions there is no longer a well defined water surface, as air is filled by water droplets and water by air bubbles; there is a continuous transition from liquid water to air with a mean density gradually changing from the density of water to the density of air, which radically changes the processes of the air/sea momentum, heat and gas exchange. These small scale processes have to be properly understood to be incorporated into operational weather forecasting and large scale circulation climate models.

THE SEA SURFACE DRAG UNDER STRONG WINDS

Wind-wave interaction at extreme wind speed is of special interest now in connection with the problem of explanation of the sea surface drag saturation at the wind speed exceeding 30 m/s. The idea on saturation (and even reduction) of the coefficient of aerodynamic resistance of the sea surface at hurricane wind speed was first suggested in by Emanuel (1995) on the basis of theoretical analysis of sensitivity of maximum wind speed in a hurricane to the ratio of the enthalpy and momentum exchange coefficients. Both field (Powel et al (2003), Jarosz et al (2007)) and laboratory (Donelan et al, (2004)) experiments confirmed that at hurricane wind speed the sea surface drag coefficient is significantly reduced in comparison with the parameterization obtained at moderate to strong wind conditions (see Fairall et al, (2003)).

Factors determining momentum exchange under high wind speeds basing on the laboratory experiment in a well controlled environment were investigated. The experiments were carried out in the Thermo-Stratified WInd-WAve Tank (TSWIWAT) of the Institute of Applied Physics. The parameters of the facility are as follows: airflow 0 - 25 m/s (equivalent 10-m neutral wind speed U10 up to 60 m/s), dimensions 10m x 0.4m x 0.7 m, temperature stratification of the water layer. Simultaneous measurements of the airflow velocity profiles and wind waves were carried out in the wide range of wind velocities. Aerodynamic resistance of the water surface was measured by the profile method at a distance of 7 m from the inlet. Wind velocity profiles were measured by the L-shaped Pitot tube with differential pressure

transducer Baratron MKS 226A with accuracy of 0.5% of full scale range i.e. 3 cm/s. Scanning method with consecutive height increment of 3 – 5 mm and accruing time of 2 minuets at each point was used. For fixed wind parameters 5 profiles were measured for subsequent averaging.

Wind friction velocity and surface drag coefficients C_{D10} were retrieved from the measurements by the profile method, the dependence of C_{D10} on U10 are shown in Figure 1. Similar to data by Donelan et al (2004) surface drag coefficient demonstrates tendency to saturation for wind speed exceeding 30 m/s.

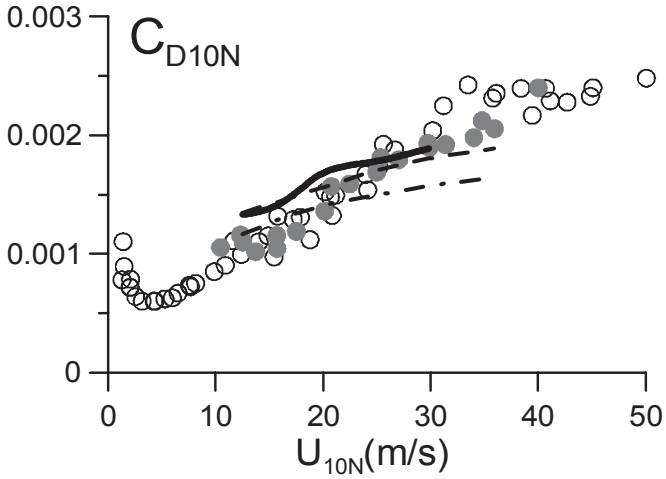

Figure 1. Surface drag coefficient via 10-m wind speed. Open circles – data from Donelan etal (2004), closed circles – data obtained at TSWIWAT, dash-dot line – theoretical calculations within quasi-linear theory (no ripples), dash line - theoretical calculations within quasi-linear theory (with ripples, model [15]), solid line - theoretical calculations within quasi-linear theory (with measured ripples)

Simultaneously with the airflow velocity measurements, the wind wave field parameters in the flume was investigated by three wire gauges positioned in corners of an equal-side triangle with 2 cm side, data sampling rate was 100 Hz. Three dimensional frequency-wave-number spectra with the wavenumbers up to 1 cm^{-1} were retrieved from this data by the algorithm similar to the wavelet directional method [12] based on window fast Fourier processing. Wave number spectra for the bandwidth 2-10cm^{-1} were measured by the optical method. The wave fields at different wind speeds are characterized by narrow wave-number spectra with the peak wave-number decreasing with the wind speed increasing. The wind-wave saturation spectra at different 10 m wind speeds U_{10} are plotted in Figure 2a. The presence of a sharp peak downshifting with the increasing wind speed and a long plato is typical for the measured spectra.

In Figure 3 we present the dependencies of the mean square slope on the wind velocity. The open circles show the mean square slope of the peak wave S_p. Other symbols present the mean square slope of the wave field calculated according to the definition:

$$Slope = \int_{k\min}^{k\max} k^2 S(k) dk , \qquad (1)$$

where $S(k)$ is the omnidirectional elevation spectrum.

Here the upper limit k_{min}=0.01 cm^{-1} was selected below the lowest wavenumber observed in the experiments. It is well known, that the integral (1) strongly depends on the upper limit k_{max}. Measurements with the array of 3 wave staffs provide $k_{max}=k_u$=1.25 cm^{-1}. The dependence $Slope(U_{10})$ for this upper limit is shown in Figure 2b by closed circles. To take into account the short wave ripples both generated near the crests of the waves due to wave breaking and excited by the wind, we continued the spectrum for $k>k_{max}$ by the model based on the ideas suggested by (Elfouhaily et al 1997). The mean square slope calculated for the composite spectrum with the upper limit k_{max}=20 cm^{-1} is shown by squares in Figure 3 as a function of U_{10}. Figure 2b clearly shows, that for both values of the upper limit k_{max} in the integral (1) the mean square slope tends to saturation when U_{10}>25 m s^{-1}. The comparison with the Figure 1 shows that

the saturation spectrum as a whole demonstrates the tendency to saturation for U_{10}>25 m s^{-1}. It means that at the wind speed about 25 m s^{-1} the regime changing of the wave field occurs. Figure 2c clearly shows linear dependence between surface drag coefficient and mean square slope. Video filming indicates onset of wave breaking with white-capping and spray generation at wind speeds approximately equal to U_{cr}.

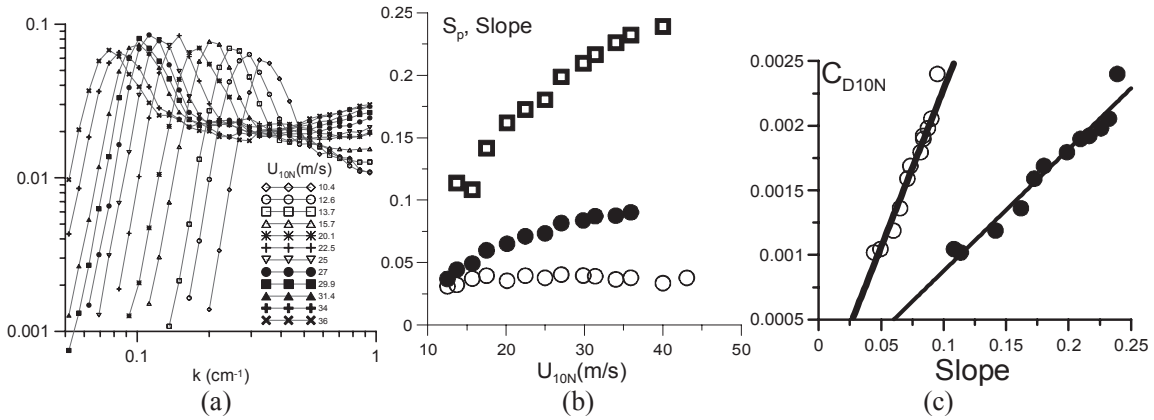

Figure 2. Saturation wave number spectrum of the waves for a definite fetch (7 m) and different wind speeds (a); dependences of the mean square slope on the wind velocity defined as (a_p k_p)/2 (open circles), the calculated accordingly integral (1) for $k_{max}=k_u$ (black circles) and k_{max}=2000 m-1 (open squares) (b); CD against mean square slope diagram. Black symbols for k_{max}=2000 m-1, open symbols for $k_{max}=k_u$ (c).

We compared the obtained experimental dependencies with the predictions of the quasi-linear model of the turbulent boundary layer over the waved water surface (Reutov, Troitskaya (1995)? Troitskaya, Rybushkina (2007)). Comparing shows that theoretical predictions give low estimates for the measured drag coefficient and wave fields (see Figure 1, dashed-dotted curve). We took into account small scale (high frequency) part of the surface roughness (k <1 см$^{-1}$). First, we add model spectrum of short from the work (Elfouhaily et al (1997)) to measured long wave part $S(k)$:

$$S_{tot}(k) = S(k) + \frac{10^{-2}}{2}\left(1+3\ln\frac{u_*}{c_m}\right)\frac{c_m}{c}e^{-\frac{1}{4}\left(\frac{k}{k_m}-1\right)^2}, c_m = 23cm/s,$$

New theoretical results are in better agreement with experiment (see. Figure 1, dashed curve). The agreement was significantly improved, when we added high-wave-number part of the wind wave spectra measured by the laser system (see Figure1, solid curve).

EFFECT OF DROPLETS ON HEAT AND MOMENTUM EXCHANGE AT STRONG WINDS

A series of experiments was carried out in the TSWIWAT IAP RAS for the study of momentum and heat exchange in a stably stratified temperature turbulent boundary layer air flow over waved surfaces. The experiments were conducted in a wide range of wind speeds and the roughness parameters (waves), including extreme with heavy wave breaking and spray.

To create a temperature stratification of the atmospheric boundary layer air entering the flume was heated to 30-40 degrees C (depending on air flow rate). The temperature of the water in all experiments was maintained constant at about 15 degrees. The studies were conducted in a wide range of wind speeds. Maximum rate on the channel axis of 8.8 m / s to 19 m / s, corresponding to an equivalent 10-m wind speed 10-35 m / s. The peculiarity of this experiment was the presence of the possibility of changing the heights of the surface waves regardless of the speed of the wind flow in the channel. For this purpose a net with thread thickness 0.25 mm and a cell of 1.6 x 1.6 mm was stretched along the channel. This net does not affect the heat exchange, but the characteristics of surface waves varied depending on the position of the grid: the waves were absent when the grid was located at the level of the undisturbed surface of the water, and the amplitude was maximal when the net was at the maximum depth 33cm.

Simultaneous measurements of velocity profiles of wind and temperature flow in the test section of the channel (at a distance of 6.5 m from the entrance to the canal) was performed using a Pitot tube with a differential pressure gauge and film hot-wire anemometer. Both sensors were mounted on the vertical scanner. The temperature and wind speed at the entrance controlled by an additional hot-wire anemometer. To measure the surface water temperature in the test section, a special temperature sensor was positioned. The average velocity and temperature profiles were obtained of the working section of the channel. By the profiling method values of friction velocity and the equivalent 10-m wind speed and the equivalent air-water temperature difference ΔT10 were obtained and their errors were estimated. As a result, the drag coefficient C_D and the water surface heat transfer coefficient C_T were calculated.

Simultaneously, the presence and number of sprays in the surface layer of air were determined. We used non-standard method of indirect estimation of the amount of the volume of spray in the air stream. It is based on the effect of a sharp decline in reading of the thermoanemometer when struck by the spray. 10-min recording was conducted at several fixed heights above the water surface. After the time series smoothing to remove hardware noise, maximum temperature value has been subtracted from the current value of the effective temperature, after which the time series was integrated. The integral was used as a marker of the amount of spray in the air flow over the waves.

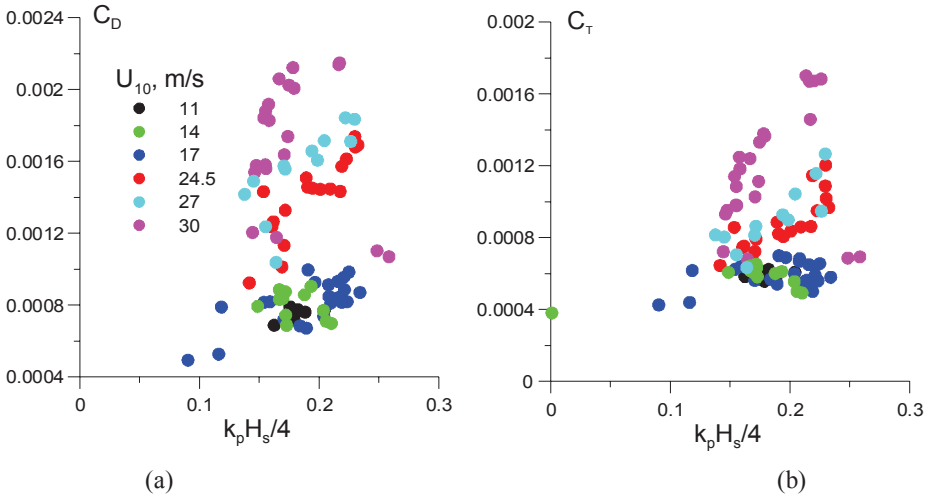

(a) (b)

Figure 3. The drag coefficient (a) and Stanton number as a function of the slope of energy-waves (b)

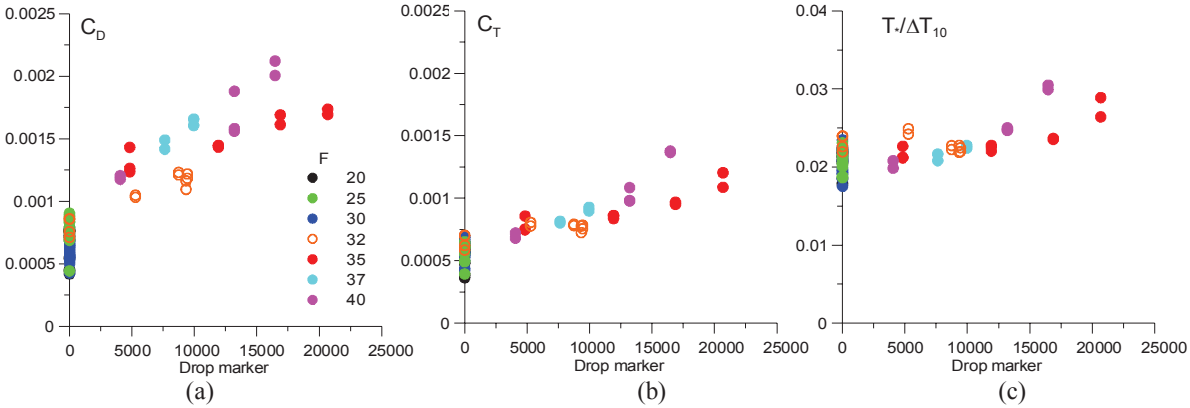

(a) (b) (c)

Figure 4 The drag coefficient (a), the number of Stanton (b) and the logarithm of the temperature roughness (c) as a function of the spray marker.

The experimental dependences of the exchange coefficients on the parameters of the air flow and wave characteristics, as well as the number of marker spray were obtained. We found that a sharp increase in the drag coefficient and Stanton numbers at wind speeds greater than 25 m / s was accompanied by the emergence and increasing concentration of the spray in the air boundary layer. (Figure 3a). The correlation coefficient between the coefficient of resistance marker and the number of sprays was close to 0.9 (Figure 4).

We suggested the hypothesis that the observed phenomenon can be explained by the phenomenon of the instability of the air and water type "bag break-up"(Villermaux, E. (2007)) (Figure 5), which was detected by the shadow method with illumination up to the light and high speed video using a high-speed camera NAC Memrecam HX-3.

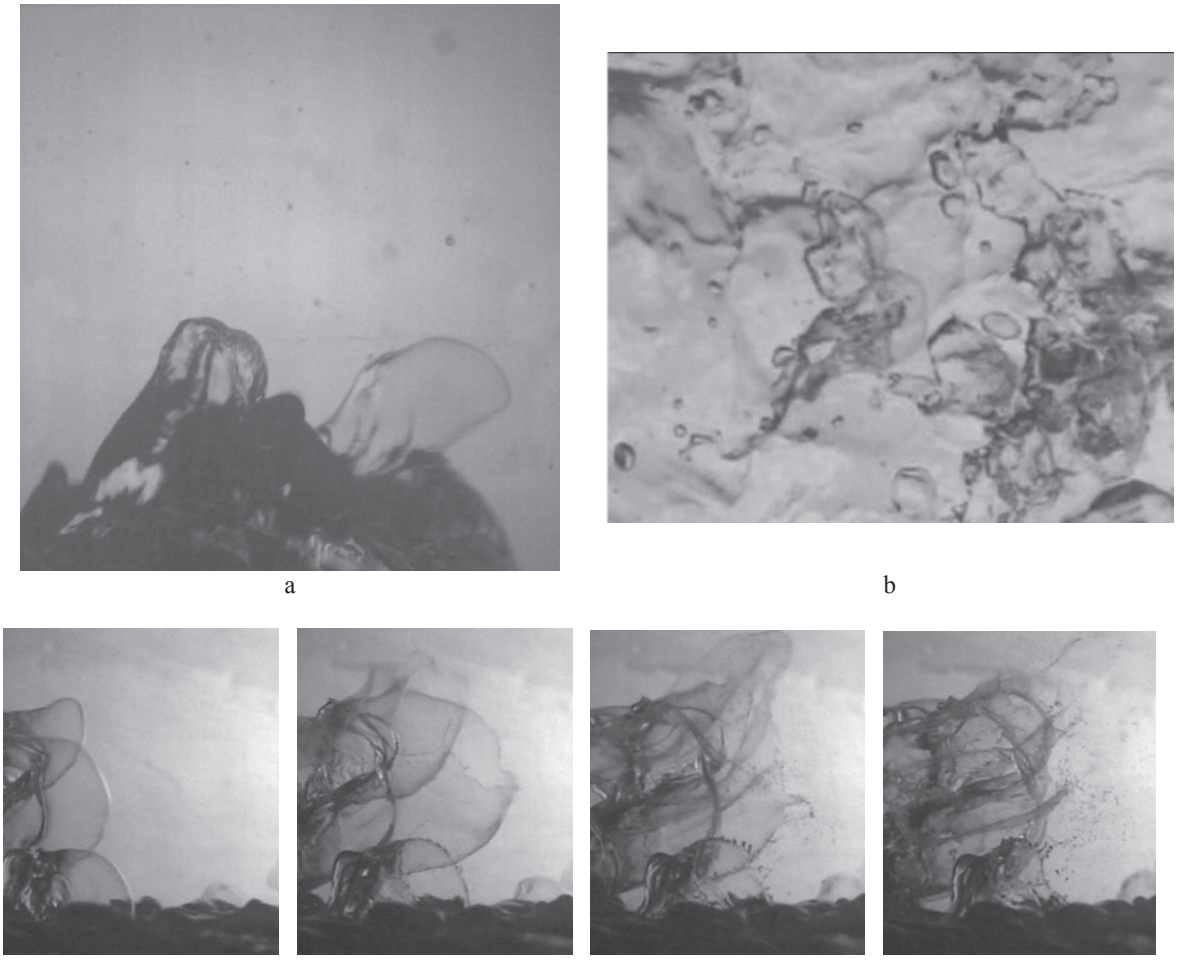

a b

Figure 5 Examples of images "membranes" side view (a) and top view (b). An example of the development of instability "membrane" to form a spray (lower panel).

CONCLUSIONS

Factors determining momentum and heat exchange under high wind speeds basing on the laboratory experiment in a well controlled environment were investigated. Basing on the experimental data a possible physical mechanism of the drag saturation at severe wind conditions is suggested. Tearing of the wave crests at severe wind conditions leads to the effective smoothing (decreasing wave slopes) of the water surface, which in turn reduces the aerodynamic roughness of the water surface. Quantitative agreement of the experimental data and theoretical estimations of the surface drag occurs if momentum flux associated with short wave part of the wind wave spectra is taken into account. A series of laboratory experiments on

modeling of wind-wave interaction in presence of stable temperature stratification surface layer of the air flow (caused by the difference between the temperature of water and air). Investigations were carried out in a wide range of wind speeds up to hurricane and wave parameters, including breaking waves. Mean velocity and temperature profiles and parameters of surface waves were measured. The dependences of the drag and heat exchange coefficients on the wind speed, wave parameters (amplitude, slope) and the values characterizing the volume of spray in the surface layer of the air flow were obtained. It was shown growth of exchange coefficients with increasing concentration of the spray. Using high-speed video revealed the dominant mechanism for the generation of spray when the wind is strong. It turned out that it is associated with the development of a special type of instability of the air and water, which is known as "bag-breakup instability" in the theory of disintegration of liquids. According to records obtained investigated the statistics of events that resulted in the spray generated in the surface layer of the atmosphere in a strong wind through the mechanism of «bag-breakup instability».

ACKNOWLEDGEMENTS

This work was supported by the Russian Foundation of Basic Research (13-05-00865, 14-05-91767, 13-05-12093, 15-05-) and Alexander Kandaurov, Maxim Vdovin and Olga Ermakova acknowledge partial support from Russian Science Foundation (Agreement No. 14-17-00667)..

REFERENCES

Emanuel, K.A. (1995) Sensitivity of tropical cyclones to surface exchange coefficients and a revised steady-state model incorporating eye dynamics. J. Atmos. Sci, Vol.52, No 22, p. 3969-3976.

Powell, M.D., Vickery P.J., Reinhold T.A. (2003) Reduced drag coefficient for high wind speeds in tropical cyclones. Nature, Vol.422, p.279-283

Jarosz E., Mitchell D. A., Wang D.W., Teague W.J. (2007) Bottom-up determination of air-sea momentum exchange under a major tropical cyclone. Science, v 315, p. 1707-1709 DOI: 10.1126/science.1136466.

Donelan M.A., Haus B.K , Reul N., Plant W.J., Stiassnie M., Graber H. C., Brown O. B., Saltzman E. S. (2004) On the limiting aerodynamic roughness of the ocean in very strong winds. *Geophys. Res. Lett*., Vol.31, L18306.

Fairall C.W., Bradley E.F., Hare J.E., Grachev A.A., Edson J.B. (2003) Bulk parameterization of air–sea fluxes: updates and verification for the COARE algorithm . J. Climate, Vol.16, No 4, p.571–591

Rikiishi, K. (1978)A new method for measuring the directional wave spectrum. Journal Physical Oceanography. Vol. 8, p. 508 – 517

Reutov, V.P. and Yu. I. Troitskaya, (1995) On the nonlinear effects in the interaction of gravity waves with turbulent airflow. Izvestiya, Atmospheric and Oceanic Physics, Vol. 31, No 6, p. 825–834

Troitskaya, Yu. I., G. V. Rybushkina. (2008) Quasi-linear model of interaction of surface waves with strong and hurricane winds. Izvestiya, Atmospheric and Oceanic Physics Vol. 44, No 5, p. 621-645

Elfouhaily T.B., Chapron B., Katsaros K., Vandemark D. (1997) A unified directional spectrum for long and short wind-driven waves // J. Geophys. Res., , v.107, p.15781–15796.

Villermaux, E. (2007) Fragmentation. Annu. Rev. Fluid Mech. 39, 419–446.